Mechanistic Studies of the Palladium-Catalyzed Amination of Aryl Halides and the Oxidative Addition of Aryl Bromides to $Pd(BINAP)_2$ and $Pd(DPPF)_2$: An Unusual Case of Zero-Order Kinetic Behavior and Product Inhibition

Luis M. Alcazar-Roman,[†] John F. Hartwig,*[,†] Arnold L. Rheingold,[‡] Louise M. Liable-Sands,[‡] and Ilia A. Guzei[‡]

Contribution from the Department of Chemistry, Yale University, P.O Box 208107, New Haven, Connecticut 06520-8107, and Department of Chemistry and Biochemistry, University of Delaware, Newark, Delaware 19716

Received December 21, 1999

Abstract: Mechanistic studies of the amination of aryl bromides catalyzed by palladium complexes containing the chelating phosphines BINAP and DPPF are reported. The coupling of primary alkyl- and arylamines, secondary cyclic alkylamines, and secondary arylalkylamines with bromoarenes in the presence of stoichiometric base and $Pd(BINAP)_2$ (**1a**) as catalyst, and the reaction of aniline with 4-Br-C_6H_4-*t*-Bu in the presence of base catalyzed by $Pd(DPPF)_2$ (**2**), were studied. The stoichiometric oxidative additions of PhBr to **1a** and to **2** were turnover limiting, and kinetic studies were also conducted on this individual step. The stoichiometric oxidative addition of PhBr to **1a** showed an inverse first-order dependence on added ligand when the PhBr concentration was low but depended solely on the rate of chelating ligand dissociation at high [PhBr]. There was no measurable solvent effect. In addition, the rates were indistinguishable in the presence and in the absence of amines and salts that are present in the catalytic amination reactions. Similar qualitative data for the oxidative addition of PhBr to **2** was obtained by ^{1}H NMR spectroscopy. The observed rate constants for the overall amination reactions catalyzed by **1a** were shown to be zero order in aryl halide, amine, base, and added ligand, while they were first order in catalyst. These data indicated that the kinetic behavior of the overall reaction was dictated solely by the rate of ligand dissociation from **1a**, as observed for the oxidative addition. When secondary amines were used, deviation from this behavior was observed. This anomalous behavior resulted from decay of catalyst rather than a change in the turnover-limiting step. A catalyst decomposition pathway that involves backbone P−C bond cleavage of the chelating bisphosphine ligands was revealed by the stoichiometric oxidative addition studies. Quantitative rate data were also obtained for reaction of 4-Br-C_6H_4-*t*-Bu with aniline in the presence of base catalyzed by **2**. The observed rate constants were zero order in amine and base, inverse first order in added ligand, and first order in aryl bromide. At low concentration of added ligand, the reaction appeared to be first order in amine. However, this deviation from the expected behavior was due to reversible reaction of the catalyst with product.

Introduction

Palladium complexes chelated by diphosphine ligands catalyze cross-coupling reactions that form C−C bonds, such as Stille,[1−4] Suzuki,[5−16] Negishi,[17] Heck,[18−30] Kumada,[17,18,31−42] and carbonyl α-arylations.[43−46] They also catalyze the recently developed conversion of aryl halides and sulfonates to amines and ethers.[47,48] Many of these cross-coupling reactions involve aryl halide or sulfonate electrophiles and are initiated by

[†] Yale University.
[‡] University of Delaware.

(1) Newhouse, B. J.; Meyers, A. I.; Sirisoma, N. S.; Braun, M. P.; Johnson, C. R. *Synlett* **1993**, 573−574.
(2) Attwood, M. R.; Raynham, T. M.; Smyth, D. G.; Stephenson, G. R. *Tetrahedron Lett.* **1996**, *37*, 2731−2734.
(3) Vedejs, E.; Haight, A. R.; Moss, W. O. *J. Am. Chem. Soc.* **1992**, *114*, 6556−6558.
(4) Segelstein, B. E.; Butler, T. W.; Chenard, B. L. *J. Org. Chem.* **1995**, *60*, 12−13.
(5) Coudret, C.; Mazenc, V. *Tetrahedron Lett.* **1997**, *38*, 5293−5296.
(6) Firooznia, F.; Gude, C.; Chan, K.; Marcopulos, N.; Satoh, Y. *Tetrahedron Lett.* **1999**, *40*, 213−216.
(7) Fuerstner, A.; Seider, G. *Tetrahedron* **1995**, *54*, 11165−11176.
(8) Fuerstner, A.; Seider, G. *Synlett* **1998**, 161−162.
(9) Gemma, E.; Lopez-Sanchez, M. A.; Martinez, M. E.; Plumet, J. *Tetrahedron* **1998**, *54*, 197−212.
(10) Kowitz, C.; Wegner, G. *Tetrahedron* **1997**, *53*, 15553−15574.
(11) Matos, K.; Soderquist, J. A. *J. Org. Chem.* **1998**, *63*, 461−470.
(12) Ruhland, B.; Bombrun, A.; Gallop, M. A. *J. Org. Chem.* **1997**, *62*, 7820−7826.
(13) Setayesh, S.; Bunz, U. H. F. *Organometallics* **1997**, *15*, 5470−5472.
(14) Vanier, C.; Wagner, A.; Mioskowski, C. *Tetrahedron Lett.* **1999**, *40*, 4335−4338.
(15) Suginome, M.; Matsuda, T.; Nakamura, H.; Ito, Y. *Tetrahedron* **1999**, *52*, 8787−8800.
(16) Nicolau, K. C.; Li, H.; Boddy, C. N. C.; Ramanjulu, J. M.; Yue, T.; Natarajan, S.; Chu, X.; Brase, S.; Rubsam, F. *Chem.-Eur. J.* **1999**, *5*, 2584−2601.
(17) Hayashi, T.; Konishi, M.; Kobori, Y.; Kumada, M.; Higuchi, T.; Hirotsu, K. *J. Am. Chem. Soc.* **1984**, *106*, 158−163.
(18) Brown, J. M.; Cooley, N. A. *Organometallics* **1990**, *9*, 353−359.
(19) Brown, J. M.; Perez-Torrente, J. J.; Alcock, N. W.; Clase, H. J. *Organometallics* **1995**, *14*, 207−213.
(20) Cabri, W.; Candiani, I.; DeBernardinis, S.; Frncalanci, F.; Penco, S.; Santo, R. *J. Org. Chem.* **1991**, *56*, 5796−5800.
(21) Olofsson, K.; Larhed, M.; Hallberg, A. *J. Org. Chem.* **1998**, *63*, 5076−5079.

10.1021/ja9944599 CCC: $19.00
Published on Web 05/02/2000

oxidative addition of the aryl halide or sulfonate to a Pd(0) complex that is typically ligated by phosphine ligands.[49−53] The resulting arylpalladium halide displays a diverse set of reactions that form organylpalladium hydrocarbyl, amido, and alkoxo complexes by transmetalation or form alkylpalladium halide complexes by olefin insertion.[53] In most cases, the "resting state" of the catalyst—in other words, the species that is the major or exclusive palladium complex in solution—is a Pd(0) phosphine complex or an arylpalladium halide complex. Thus, the rate of oxidative addition often dictates the overall rate of the catalytic reaction, and the rate of decomposition of an arylpalladium halide complex can dictate turnover numbers and catalyst stability.

Many studies on the oxidative addition of aryl halides to zerovalent palladium complexes of triphenylphosphine and other monophosphines have been published.[49,50,52,54] However, few studies have addressed the oxidative addition of aryl halides to palladium complexes supported by chelating phosphines.[51,55,56] In particular, only one study presents the oxidative addition of aryl halides to Pd(0) ligated by chelating phosphines, such as [1,1′-bis(diphenylphosphino)ferrocene (DPPF) and 2,2′-bis-(diphenylphosphino)-1,1′-binaphthyl (BINAP), which are particularly useful ligands for the catalytic amination of aryl halides.[51] The published work involves the oxidative addition of aryl halides to palladium complexes supported by ligands that are generated in situ and that are ligated by both alkenes, such as methyl acrylate or *trans*,*trans*-dibenzylideneacetone (DBA), and either DPPF or BINAP. While these data are useful for cases in which the catalyst is generated from $Pd_2(DBA)_3$ or $Pd(DBA)_2$ as a zerovalent palladium source, they are less informative when $Pd(OAc)_2$ or other species are used to generate the active catalyst. Moreover, we have observed that DBA can be consumed in the catalytic reaction, generating homoleptic phosphine palladium complexes as the resting state even when $Pd_n(DBA)_m$ is used as the catalyst precursor.

Since the palladium-catalyzed amination of aryl halides with tin amides was reported by Kosugi and Migita, aryl halide amination has become a general, synthetically valuable route to arylamines.[47,57−72] Work in the authors' laboratory and in Buchwald's laboratory has allowed for the use of amines and base instead of tin amides and has led to improvements in selectivity, scope of suitable substrates, and catalyst stability. The complexes formed from a palladium precursor and the chelating phosphines DPPF or BINAP (Scheme 1) are more effective catalysts for the arylation of primary amines than the original catalysts bearing P(*o*-tolyl)$_3$ as ligand.[47,48]

Some of the stoichiometric reactions involved in the arylation of amines using these chelating ligands have been studied, but the initial oxidative addition step involving these catalysts has not been investigated. Moreover, the kinetic behavior of the overall catalytic system is unknown. The catalytic cycle is certainly initiated by the oxidative addition of an aryl bromide to a Pd(0) complex to form a cis arylpalladium bromide complex that is ligated by either DPPF or BINAP. This aryl bromide

(22) Ashimori, A.; Bachand, B.; Calter, M. A.; Govek, S. P.; Overman, L. E.; Poon, D. J. *J. Am. Chem. Soc.* **1998**, *120*, 6488−6499.
(23) Ashimori, A.; Bachand, B.; Overman, L. E.; Poon, D. J. *J. Am. Chem. Soc.* **1998**, *120*, 6477−6487.
(24) Kondo, K.; Sodeoka, M.; Mori, M.; Shibasaki, M. *Tetrahedron Lett.* **1993**, *34*, 4219−4222.
(25) Oshima, T.; Kegechika, K.; Adachi, M.; Sodeoka, M.; Shibasaki, M. *J. Am. Chem. Soc.* **1996**, *118*, 7108−7116.
(26) Kurihara, Y.; Sodeoka, M.; Shibasaki, M. *Chem. Pharm. Bull.* **1994**, *42*, 2357−2359.
(27) Sato, Y.; Sodeoka, M.; Shibasaki, M. *Chem. Lett.* **1990**, 1953−1954.
(28) Sato, Y.; Sodeoka, M.; Shibasaki, M. *J. Org. Chem.* **1989**, *54*, 4738−4739.
(29) Takemoto, T.; Sodeoka, M.; Sasai, H.; Shibasaki, M. *J. Am. Chem. Soc.* **1993**, *115*, 8477−8478.
(30) Tietze, L. F.; Raschke, T. *Synlett* **1995**, 597−598.
(31) Bumagin, N. A.; Andryukhova, N. P.; Beletskaya, I. P. *Dokl. Akad. Nauk SSSR* **1987**, *297*, 1126−1129.
(32) Bumagin, N. A.; Angryukhova, N. P.; Beletskaya, I. P. *Metalloorg. Khim.* **1989**, *2*, 893−897.
(33) Bumagin, N. A.; Sikolova, A. F.; Beletskaya, I. P. *Izv. Akad. Nauk, Ser. Khim.* **1993**, 2009−2010.
(34) Bumagin, N. A.; Safarov, F. S.; Beletskaya, I. P. *Dokl. Akad. Nauk* **1993**, *332*, 48−49.
(35) Bumagin, N. A.; Luzikova, E. V.; Beletskaya, I. P. *Zh. Org. Khim.* **1995**, *31*, 1663−1666.
(36) Bumagin, N. A.; Sokolova, A. A.; Beletskaya, I. P.; Wolz, G. *Zh. Org. Khim.* **1993**, *29*, 162−164.
(37) Flandanese, V.; Miccoli, G.; Naso, F.; Ronzini, L. *J. Organomet. Chem.* **1986**, *312*, 343−348.
(38) Hayashi, T.; Konishi, M.; Kumada, M. *Tetrahedron Lett.* **1979**, *21*, 1871−1874.
(39) Katayama, T.; Umeno, M. *Chem. Lett.* **1991**, 2073−2076.
(40) Kranenburg, M.; Kamer, P. C. J.; Van Leeuween, P. W. N. M. *Eur. J. Inorg. Chem.* **1998**, 155−157.
(41) Rehm, J. D. D.; Ziemer, B.; Sziemies, G. *Eur. J. Org. Chem.* **1999**, 2079−2085.
(42) Rozenberg, V. I.; Sergeeva, E. V.; Kharitonov, V. G.; Vorontsova, N. V.; Vorontsova, E. V.; Mikul'shina, V. V. *Izv. Akad. Nauk, Ser. Khim.* **1994**, 1081−1085.
(43) Hamann, B. C.; Hartwig, J. F. *J. Am. Chem. Soc.* **1997**, *119*, 12382.
(44) Shaughnessy, K. H.; Hamann, B. C.; Hartwig, J. F. *J. Org. Chem.* **1998**, *63*, 6546.
(45) Ahman, J.; Wolfe, J. P.; Troutman, M. V.; Palucki, M.; Buchwald, S. L. *J. Am. Chem. Soc.* **1998**, *120*, 1918−1919.
(46) Palucki, M.; Buchwald, S. L. *J. Am. Chem. Soc.* **1997**, *119*, 11108−11109.
(47) Driver, M. S.; Hartwig, J. F. *J. Am. Chem. Soc.* **1996**, *118*, 7217.
(48) Wolfe, J. P.; Wagaw, S.; Buchwald, S. L. *J. Am. Chem. Soc.* **1996**, *118*, 7215−7216.
(49) Amatore, C.; Pflüger, F. *Organometallics* **1990**, *9*, 2276−2282.
(50) Amatore, C.; Jutand, A.; M'Barki, M. A. *Organometallics* **1992**, *11*, 3009−3013.
(51) Amatore, C.; Broeker, G.; Jutand, A.; Khalil, F. *J. Am. Chem. Soc.* **1997**, *119*, 5176−5185.
(52) Amatore, C.; Jutand, A.; Suarez, A. *J. Am. Chem. Soc.* **1993**, *115*, 9351−9541.
(53) Collman, J. P.; Hegedus, L. S.; Norton, J. R.; Finke, R. G. *Principles and Applications of Organotransition Metal Chemistry*, 2nd ed.; Wiley-Interscience: New York, 1987; p 322−333.
(54) Hartwig, J. F.; Paul, F. *J. Am. Chem. Soc.* **1995**, *117*, 5373−5374.
(55) Portnoy, M.; Milstein, D. *Organometallics* **1993**, *12*, 1665−1673.
(56) Jutand, A.; Hii, K. K. M.; Thornton-Pett, M.; Brown, J. M. *Organometallics* **1999**, *18*, 5367−5374.
(57) Kosugi, M.; Kameyama, M.; Sano, H.; Migita, T. *Nippon Kagaku Kaishi* **1985**, *3*, 547−551.
(58) Kosugi, M.; Kameyama, M.; Migita, T. *Chem. Lett.* **1983**, 927−928.
(59) Yang, B. H.; Buchwald, S. L. *J. Organomet. Chem.* **1999**, *576*, 125−146.
(60) Wolfe, J. P.; Wagaw, S.; Marcoux, J. F.; Buchwald, S. L. *Acc. Chem. Res.* **1998**, *31*, 805−818.
(61) Hartwig, J. F. *Angew. Chem., Int. Ed.* **1998**, *37*, 2047−2067.
(62) Hartwig, J. F. *Acc. Chem. Res.* **1998**, *31*, 852−860.
(63) Hamann, B. C.; Hartwig, J. F. *J. Am. Chem. Soc.* **1998**, *120*, 7369−7370.
(64) Hartwig, J. F.; Kawatsura, M.; Hauck, S. I.; Shaughnessy, K. H.; Alcazar-Roman, L. M. *J. Org. Chem.* **1999**, *64*, 5575−5580.
(65) Old, D. W.; Wolfe, J. P.; Buchwald, S. L. *J. Am. Chem. Soc.* **1998**, *120*, 9722−9723.
(66) Bei, X.; Uno, T.; Norris, J.; Turner, H. W.; Weinberg, W. H.; Guram, A. S.; Petersen, J. L. *Organometallics* **1999**, *18*, 1840−1853.
(67) Bei, X.; Turner, H. W.; Weinberg, W. H.; Guram, A. S.; Petersen, J. L. *J. Org. Chem.* **1999**, *64*, 6797−6803.
(68) Bei, X. H.; Uno, T.; Norris, J.; Turner, H. W.; Weinber, W. H.; Guram, A. S.; Petersen, J. L. *Organometallics* **1999**, *18*, 1840−1853.
(69) Bei, X. H.; Creiver, T.; Guram, A. S.; Jandeleit, B.; Powers, T. S.; Turner, H. W.; Uno, T.; Weinberg, W. H. *Tetrahedron Lett.* **1999**, *40*, 3855−3858.
(70) Bei, X. H.; Guram, A. S.; Turner, H. W.; Weinberg, W. H. *Tetrahedron Lett.* **1999**, *40*, 1237−1240.
(71) Reddy, N. P.; Tanaka, M. *Tetrahedron Lett.* **1997**, *38*, 4807−4810.
(72) Wolfe, J. P.; Buchwald, S. L. *Angew. Chem., Int. Ed.* **1999**, *36*, 7026−7033.

Scheme 1

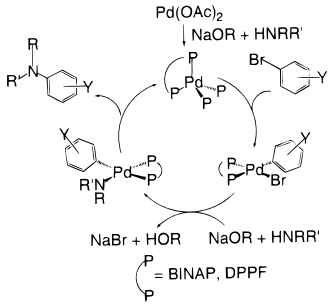

complex is transformed into the cis arylpalladium amido complex by base and amine. Reductive elimination forms the final arylamine product. Because of the absence of mechanistic data on the initial step and the overall cycle, it is not clear which steps are reversible, which step is irreversible and turnover limiting, and whether product coordination can inhibit reaction rates. Moreover, potential pathways for catalyst decomposition are unknown. For these reasons, we have conducted a kinetic study of the catalytic amination of aryl bromides and of the first step in the catalytic cycle, the oxidative addition of aryl bromides to $Pd(DPPF)_2$ and $Pd(BINAP)_2$.

We report the identification of bis-BINAP and bis-DPPF Pd(0) complexes as the dominant resting state in the catalytic cycle for the amination of aryl bromides and the identification of free Pd(chelate) as the intermediate that undergoes oxidative addition of the aryl halide. The activity of $Pd(chelate)_2$ toward oxidative addition of aryl halides conflicts with that reported by Amatore.[51] Further, our studies on the stability of arylpalladium halide complexes revealed a pathway for decomposition of palladium aryl halide complexes containing DPPF and BINAP as ligand. This decomposition pathway generates monodentate ligands and could, therefore, have an impact on catalyst selectivity and activity. Moreover, catalyst decomposition and product inhibition provide unexpected kinetic behavior with some amine substrates.

Results

Synthesis and X-ray Structural Study of (Chelate)$_2$Pd(0) Complexes. Preliminary experiments in our laboratory suggested that the resting state of the palladium catalyst was a palladium(0) complex. Thus, we prepared the homoleptic palladium(0) complexes of DPPF and BINAP. One published synthesis of Pd(BINAP)$_2$ (**1a**) involves reaction of (η-Cp)Pd(η-allyl) and (*R*)-BINAP and recrystallization of the product from CH_2Cl_2 and ether. We prepared $Pd(BINAP)_2$ in 87% isolated yield by the addition of 2 equiv of either resolved or racemic BINAP to $Pd[P(o\text{-}Tol)_3]_2$ in benzene. Only one $^{31}P\{^1H\}$ resonance at 27.4 ppm was observed for the product in all cases, indicating that Pd[(*R*)-BINAP][(*S*)-BINAP] is not formed or, less likely, that its $^{31}P\{^1H\}$ resonance is indistinguishable from those of Pd[(*R*)-BINAP]$_2$ and Pd[(*S*)-BINAP)]$_2$. Pd[(*R*)-Tol-BINAP]$_2$ (**1b**) was prepared similarly, and it was isolated in 66.8% yield as single crystals after the reaction mixture was layered with pentane. An ORTEP diagram of **1b** is provided in Figure 1. This structure can be described as a distorted tetrahedron. The two P−Pd−P angles containing phosphorus atoms of the same (*R*)-Tol-BINAP ligand are 90.87(9)° and 90.84(9)°. The other two P−Pd−P angles are 122.79(9)° and 120.31(9)°.

The synthesis of $Pd(DPPF)_2$ (**2**) was less straightforward. There are conflicting reports about the preparation of this compound. Amatore[51] and Hor[73] reported the borohydride reduction of $(DPPF)PdCl_2$ in the presence of DPPF to form a cream-colored solid that does not oxidatively add iodobenzene at room temperature.[51] Broadwood-Strong prepared light yellow $Pd(DPPF)_2$ by displacement of ethylene in $(DPPE)Pd(C_2H_4)$ by excess DPPF.[74] We generated $Pd(DPPF)_2$ as a yellow powder by reacting 2 equiv of DPPF with $Pd[P(o\text{-}Tol)_3]_2$ in benzene. The same $^{31}P\{^1H\}$ chemical shift of 7.5 ppm as for the previous yellow material was observed, but the sample contained two impurities. One of these was identified as free DPPF, and the second was assigned the dinuclear structure $[(DPPF)Pd]_2(\mu\text{-DPPF})$ (**3**), due to its doublet and triplet $^{31}P\{^1H\}$ NMR resonances in a 2:1 ratio. We were unable to obtain pure bulk samples of **3**, but a single crystal was selected and the structure was confirmed by X-ray analysis. An ORTEP diagram of **3** is shown in Figure S1 (Supporting Information). This synthetic work suggested that the two complexes existed in equilibrium. This assertion was demonstrated by addition of small amounts of $Pd[P(o\text{-}Tol)_3]_2$ to a solution of DPPF in THF. When DPPF is present in excess amounts, a singlet resonance for coordinated ligand in **2** was observed. After addition of greater than 0.5 equiv of $Pd[P(o\text{-}Tol)_3]_2$, doublet and triplet signals due to **3** were observed. Further addition of $Pd[P(o\text{-}Tol)_3]_2$ led to increasing amounts of **3** at the expense of **2**.

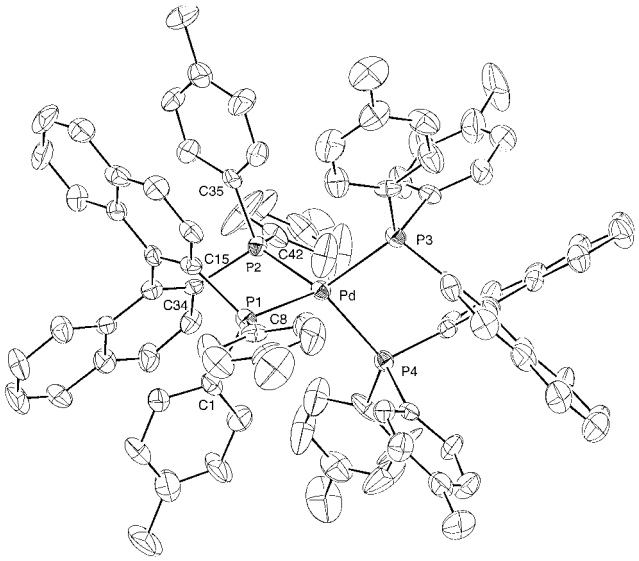

Figure 1. ORTEP drawing of Pd[(*R*)-Tol-BINAP]$_2$.

Identification of the Catalyst Resting State. To determine the resting state of the palladium catalyst for various amination reactions, we conducted catalytic reactions with amine and either bromobenzene or 4-Br-C_6H_4-*t*-Bu and sodium *tert*-butoxide base in the presence of 10 mol % of catalyst in toluene solvent. Reactions catalyzed by DPPF-ligated palladium were initiated by a combination of (DPPF)Pd(4-C_6H_4-*t*-Bu)Br (**4**) and DPPF. Reactions catalyzed by BINAP-ligated palladium were initiated by **1a**. The only species observed by $^{31}P\{^1H\}$ NMR spectroscopy for the reaction of primary amines with bromobenzene catalyzed by BINAP-ligated palladium was $Pd(BINAP)_2$. Reactions containing P(*o*-tolyl)$_3$ as internal standard showed less than 15% loss of $Pd(BINAP)_2$ at the end of the reaction. The only species observed by $^{31}P\{^1H\}$ NMR spectroscopy for reaction of aniline and 4-Br-C_6H_4-*t*-Bu catalyzed by DPPF-ligated palladium at early reaction times was Pd(0) complex **2**. The identity of the resting state for other reactions was less straightforward and will be discussed below. These data suggest that oxidative

(73) Fang, Z.; Low, P. M. N.; Ng, S.; Hor, T. S. A. *J. Organomet. Chem* **1994**, *483*, 17−20.

(74) Broadwood-Strong, G. T. L.; Chaloner, P. A.; Hitchcock, P. B. *Polyhedron* **1993**, *12*, 721−729.

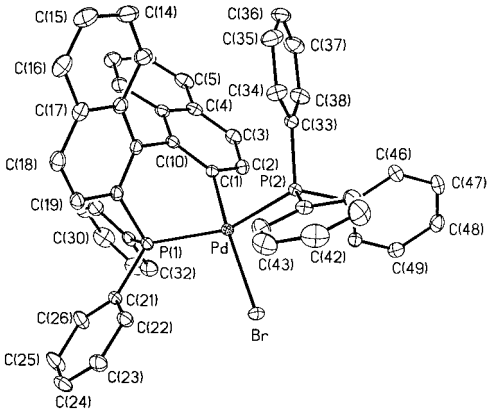

Figure 2. ORTEP drawing of the backbone P−C cleavage product **6**.

Scheme 2

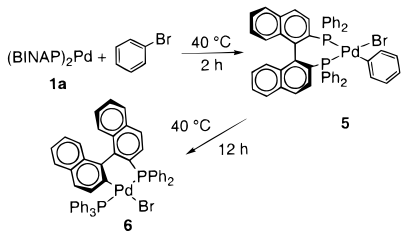

addition is turnover limiting. When the convenient mixture of $Pd(OAc)_2$ and 1−2 equiv of BINAP or DPPF as catalyst was used, **1a** and **2** formed within minutes after addition of amine and base and heating in the NMR spectrometer probe at 75 °C. In contrast to observations made on the asymmetric Heck reaction using BINAP as ligand, there was no detectable resonance for the monoxide of either BINAP or DPPF.[50,75,76]

Reactions of (Chelate)$_2$Pd(0) Complexes with Aryl Bromides. The observation of $(chelate)_2Pd(0)$ complexes as the resting state prompted us to study the oxidative addition of aryl bromides to BINAP complex **1a** and DPPF complex **2**. The reaction of 4-bromobenzaldehyde with **1a** occurred in 99% yield as determined by ^{1}H NMR spectroscopy employing an internal standard. The addition of PhBr to **2** occurred in 89% yield, in contrast to previous assertions that $Pd(DPPF)_2$ does not react with aryl halides.[51] The oxidative addition of bromobenzene to **1a** was less straightforward. Heating **1a** in the presence of 5 equiv of PhBr at 65 °C produced (BINAP)Pd(Ph)(Br) (**5**) at initial stages of the reaction, but signals due to **5** decayed during later stages and were replaced by two doublets with a trans J_{PP} value due to two mutually trans phosphine ligands. The material corresponding to these signals, complex **6** in Scheme 2 and Figure 2, contains a coordinated PPh_3 and a palladacyclic structure. Palladacyclic complex **6** displays a small dihedral angle between the naphthyl groups of 51° and displays severe deviations from ideal geometry at the metal. The square plane is distorted into a saddle shape, with each pair of trans substituents bent out of the plane in opposite directions. Complex **6** is formed by P−C bond cleavage of the ligand backbone in (BINAP)Pd(Ph)(Br). The P−C cleavage reaction was also observed with pure **5** prepared by the reaction of $\{Pd[P(o\text{-}Tol)_3](Ph)(\mu\text{-}Br)\}_2$ (**7**) with BINAP. The P−C cleavage process was accelerated in more polar solvents, such as THF or DMA.

The formation of the analogous product from backbone P−C bond cleavage of [(DPPF)Pd(Ph)(Br)] was identified spectroscopically after heating of [(DPPF)Pd(Ph)(Br)] at 130 °C in toluene-d_8 or xylenes for 18 h. In DMA solvent, this reaction occurred in 6 h at 100 °C. These two reactions constitute an unusual type of P−C bond cleavage and make it possible that the palladacyclic materials could be produced during catalytic reactions in which there is a substantial lifetime of the aryl halide complex. Although the reaction of the DPPF complex occurred less rapidly than that of [(BINAP)Pd(Ph)(Br)], this ligand transformation could be important for reactions involving [(DPPF)Pd(Ar)(Br)] at high temperatures in polar solvents.

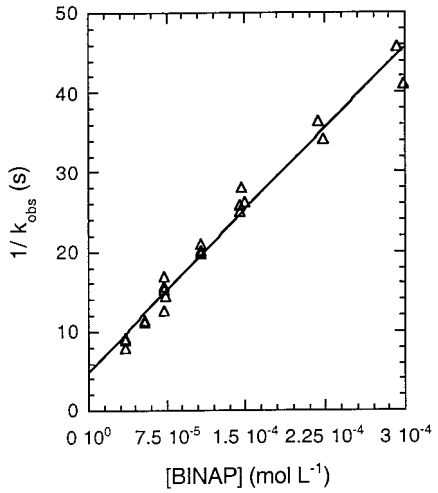

Figure 3. Determination of the order in BINAP for the oxidative addition of PhBr to **1a**.

Mechanism of Aryl Halide Oxidative Addition to Pd(Chelate)$_2$. Although BINAP-ligated aryl halide complex **5** is unstable toward backbone cleavage and aryl group exchange, this instability does not affect the rate of oxidative addition of aryl halides to Pd(0) **1a**. Complex **1a** displays a metal-to-ligand charge-transfer band centered at 520 nm, which gives it its deep wine red color. Due to the difficulty in isolating pure DPPF complex **2**, the stoichiometric oxidative addition to this material was studied qualitatively; detailed studies were conducted on the catalytic cycle as described in a later section.

Rate constants for oxidative addition were obtained at 45 °C by UV−vis spectroscopy of reactions that contained a concentration of **1a** of 2.26×10^{-5} M, concentrations of aryl bromide between 1.78×10^{-3} and 8.95×10^{-2} M, and concentrations of BINAP ranging from 3.60×10^{-5} to 2.98×10^{-4} M. A typical kinetic plot for the decay of **1a** is given in Figure S2. The dependence of the reaction rate constant on [BINAP] was measured using a constant concentration of [PhBr] equal to 1.78×10^{-3} M. A plot of $1/k_{obs}$ versus [BINAP] is shown in Figure 3. The dependence of reaction rate on [PhBr] was measured with a constant 5.40×10^{-4} M concentration of BINAP (Figure 4 and double reciprocal plot in Figure S3). Figure 4 illustrates that the measured rate constant displays saturation behavior at high concentrations of [PhBr]. At 1.78×10^{-3} M concentration of PhBr, reaction rates were within 8% of each other in benzene, toluene, THF, and 2,5-dimethyl−THF solvent (Table 1). Reactions with structurally diverse ortho-substituted aryl halides were conducted using a concentration of 8.9×10^{-1} M aryl halide, which is in the region of the curve in Figure 4 that should display zero-order behavior in [ArBr]. The values of k_{obs} for reaction of 2-bromoanisole, 2-bromotoluene, and 2-bromo-*p*-xylene all showed rate constants that were within experimental error of that for the addition of bromobenzene to **1a** (Table 2). Rate constants obtained in the presence of tetradecylamine and Bu_4NPF_6 in THF solvent were indistinguishable from those obtained

(75) Grushin, V. V. *J. Am. Chem. Soc.* **1999**, *121*, 5831−5832.
(76) Ozawa, F.; Kubo, A.; Matsumoto, Y.; Hayashi, T. *Organometallics* **1993**, *12*, 4188−4196.

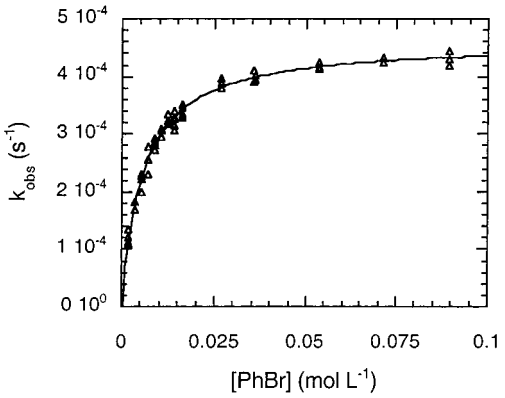

Figure 4. Plot of the observed rate constant vs concentration of PhBr for the oxidative addition of PhBr by **1a**.

Table 1. Solvent Effect on the Oxidative Addition of PhBr to **1a**

solvent	k_{obs} ($\times 10^{-5}$ s^{-1})
benzene	9.9
THF	7.3
toluene	8.1
2,5-dimethyl-THF	7.2

Table 2. Rate Constants for Oxidative Addition of Different Aryl Bromides to **1a**

aryl bromide	k_{obs} ($\times 10^{-4}$ s^{-1})
2-bromoanisole	3.9
2-bromo-*p*-xylene	4.4
2-bromotoluene	4.0

in their absence. Reactions run in the presence of NaO^{t}Bu deviated from first-order behavior due to the reaction of the oxidative addition product (BINAP)Pd(Ph)Br with alkoxide to re-form Pd(0) and generate arenes, biaryls, and small amounts of *tert*-butyl aryl ethers.[77] The oxidative addition rate constant at 60 °C in the saturation region of Figure 4 with [**1a**] equal to 2.26×10^{-5} M, [BINAP] equal to 5.40×10^{-4} M, and [PhBr] equal to 8.95×10^{-2} M was 3.4×10^{-3} s^{-1}, which is roughly an order of magnitude greater than the rate measured at 45 °C ($(4.3 \pm 0.13) \times 10^{-4}$ s^{-1}).

Although not measured quantitatively, the oxidative addition of PhBr to DPPF complex **2** showed a similar inverse dependence on phosphine concentration and positive rate dependence on [ArBr]. However, saturation of the observed rate constant at high [ArBr] was not observed. Even at concentrations of ArBr as high as 0.1 M, the reaction showed a positive dependence on [ArBr] and an inverse dependence on [DPPF].

Kinetic Behavior of the Catalytic Reactions. In general, the kinetic behavior of a catalytic cycle is dictated by the kinetic behavior of the turnover-limiting stoichiometric reaction if this reaction lies directly on the catalytic cycle. In this case, the rate law for the reaction of the resting state of the catalyst with substrate is identical to that of the catalytic system if the reaction of the resting state is irreversible. However, several differences between stoichiometric and catalytic reactions can be observed. For example, the resting state may not lie on the catalytic cycle, catalysts can decompose, products can inhibit reactions, and reaction byproducts or additives can affect the rate of the turnover-limiting step.

Thus, we sought to determine if the kinetic behavior of the palladium-catalyzed amination could be simply predicted from the kinetics of the oxidative addition. In particular, the zero-order rate behavior in [ArBr] for the oxidative addition reaction at large ratios of [ArBr]/[BINAP] should provide an unusual kinetic situation for the overall catalytic process. The catalytic reactions contain a much larger concentration of substrate than free ligand, creating a system that would show zero-order rate behavior in aryl bromide, ligand, and all substrates that react after the turnover-limiting step. Thus, the rate of the catalytic cycle should depend only on the concentration of catalyst. We conducted studies on the reaction of aryl halides with primary alkylamines catalyzed by Pd(BINAP)$_2$ as catalyst to test these predictions. In addition, we studied the arylation of aniline using (DPPF)Pd(4-C$_6$H$_4$-*t*-Bu)Br as catalyst to determine if the qualitative behavior of aryl bromide oxidative addition to Pd(DPPF)$_2$ would be observed in quantitative rate studies on the catalytic system. Both of these reactions occur in high yield. Reactions of secondary alkylamines with aryl halides using either catalyst gave variable yields of *N*,*N*-dialkylarylamines. Thus, we also studied the kinetics of the addition of *N*-methylaniline, *N*-methylpiperazine, piperidine, and morpholine to phenyl bromide catalyzed by Pd(BINAP)$_2$.

Table 3. Rate Constants for Reaction of Amines with Bromobenzene Catalyzed by **1a**

amine	k_{obs} ($\times 10^{-5}$ s^{-1} mol^{-1} L)
hexylamine	3.2
sec-butylamine	3.1
benzylamine	2.8
p-anisidine	3.0
aniline	2.3

Kinetic Behavior of Reactions of Primary Amines with Aryl Halides. When Pd(BINAP)$_2$ was used as catalyst, the reactions were typically conducted at 60 °C with the soluble alkoxide base NaOC(Et)$_3$, added BINAP, bromobenzene, and an internal standard (ferrocene or 1,3,5-trimethoxybenzene) in benzene-d_6. Final concentrations of the reaction components were 1.25 mM Pd(BINAP)$_2$, 1.25−7.98 mM BINAP, 0.1363−0.500 M NaOC(Et)$_3$, and 0.800−1.60 M PhBr and 12.6 mM amine. The reactions were monitored by ^{1}H NMR spectroscopy. Both decay of amine and appearance of product were monitored when possible. Monitoring of the reactions of primary amines by ^{31}P{^{1}H} NMR spectroscopy showed that no appreciable consumption of catalyst **1a** occurred (Figure S4). There was at most a decrease of 15% of the intensity of the resonance corresponding to **1a** vs internal standard (P[*o*-Tol]$_3$) during this reaction.

Linear plots of concentration of starting material vs time were obtained for reactions of hexylamine, *sec*-butylamine, benzylamine, *p*-anisidine, and aniline (Figure S5 for hexylamine). These data demonstrate that the reactions are zero order in amine. Moreover, all amines, with the single exception of aniline, gave reaction rates that were within experimental error of the rate obtained from hexylamine (Table 3). The rate obtained when aniline was used under the same reaction conditions was roughly 75% of the magnitude of the rates obtained for reactions of other amine substrates. The reaction was determined to be zero order in [BINAP], [PhBr], and [NaOC(Et)$_3$] by conducting experiments with the concentration of reagents in the ranges provided above (Table 4).

Kinetic Behavior of Reactions of Secondary Amines with Aryl Halides. Reactions employing the secondary cyclic amines morpholine, piperidine, and *N*-methylpiperazine and the reaction employing the acyclic secondary amine *N*-methylaniline displayed plots of amine concentration versus time that resembled plots of a reaction that was first order in amine (Figure 5). In some cases, starting amine remained after long reaction times.

(77) Mann, G.; Hartwig, J. F. *J. Am. Chem. Soc.* **1996**, *118*, 13109−13110.

Table 4. Rate Constants for Reaction of Hexylamine with Bromobenzene Catalyzed by **1a**, as a Fucntion of Bromobenzene, BINAP, and Base Concentrations

[BINAP] (mM)	k_{obs} ($\times 10^{-5}$ s^{-1} mol^{-1} L)	[ArBr] (M)	k_{obs} ($\times 10^{-5}$ s^{-1} mol^{-1} L)	[NaOR] (M)	k_{obs} ($\times 10^{-5}$ s^{-1} mol^{-1} L)
1.3	3.2	0.800	3.2	0.136	3.2
2.6	3.2	1.000	2.7	0.200	3.0
4.0	3.1	1.200	2.8	0.300	2.9
5.3	2.6	1.400	2.7	0.400	3.4
6.6	3.0	1.600	3.0	0.500	2.9
8.0	3.1				

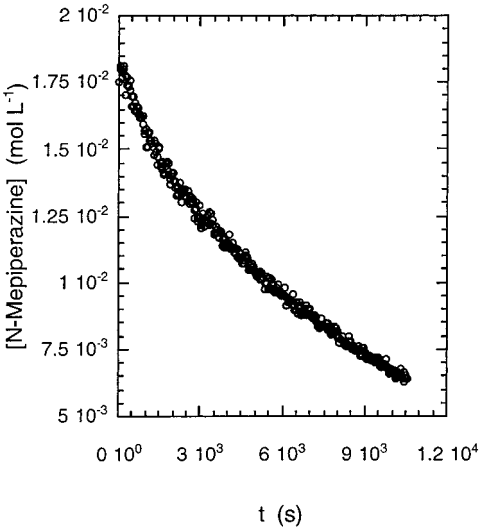

Figure 5. Decay of *N*-methylaniline during the reaction of *N*-methylaniline with bromobenzene catalyzed by **1a**.

At first glance, these data suggest a change in resting state to one that reacts with amine.

To determine if the resting state had indeed changed, we assessed whether oxidative addition was faster than the steps that follow it in the catalytic cycle when secondary amine substrates were used. Reaction of lithium morpholide with a mixture of **5** and BINAP (Pd/L ratio 1:2) gave *N*-phenylmorpholine rapidly at room temperature in high yield. The reaction of morpholine and $NaOC(Et)_3$ with **5** and ligand also showed the rapid formation of *N*-phenylmorpholine without the formation of any intermediate with a lifetime long enough to detect by $^{31}P\{^1H\}$ NMR spectroscopy. Thus, oxidative addition is much slower than the reaction of any arylpalladium(II) intermediates with amine or base, and the resting state should be a Pd(0) complex and not a species that reacts with amine.

These apparently conflicting data were explained by careful examination of the concentration of $Pd(BINAP)_2$ during the catalytic reactions. In contrast to results from monitoring the reactions of primary amines catalyzed by **1a**, monitoring of the reaction between *N*-methylaniline and bromobenzene by $^{31}P\{^1H\}$ NMR spectroscopy using P(*o*-tolyl)$_3$ as an internal standard revealed that **1a** was gradually consumed (Figure S6). Thus, the reduction of reaction rate with conversion was due to catalyst decomposition, not to a change in resting state and a resulting rate dependence on amine.

This consumption of **1a** generated free BINAP and small amounts of other phosphorus-containing compounds. Addition of DMPE to the reaction solution to liberate coordinated arylphosphines generated several new $^{31}P\{^1H\}$ NMR resonances, one of which was identical to that of free 2-diphenylphosphino-1,1′-binaphthyl,[78] which would be formed by the backbone cleavage process described above. Unfortunately, ^1H NMR

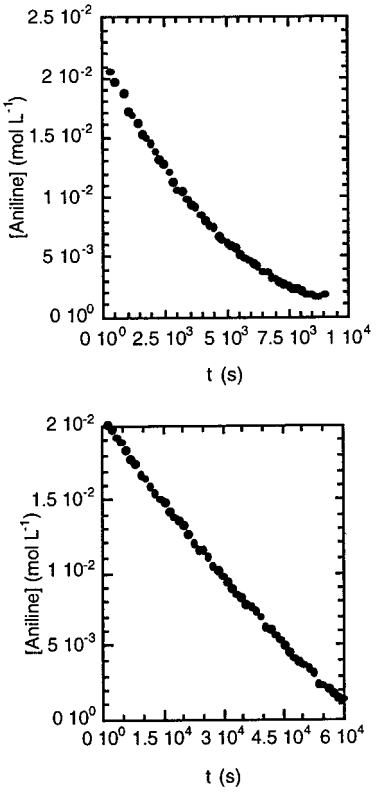

Figure 6. Decay of aniline during its reaction with bromobenzene catalyzed by **2**. [DPPF] = 2.0 mM (inset) and [DPPF] = 21.6 mM.

spectra of the aromatic region contained too many components to determine unambiguously that this material was present. The backbone P−C cleavage is one of several decomposition pathways to form catalytically inactive, homogeneous products. No black palladium-containing material precipitated.

Kinetic Studies of Reactions Catalyzed by Pd(DPPF)$_2$. Quantitative rate studies on the reaction of aniline with 4-Br-C_6H_4-*t*-Bu were conducted at 60 °C on samples containing 2.0 mM [(DPPF)Pd(4-C_6H_4-*t*-Bu)Br], 4.0−38.9 mM DPPF, 0.800−3.200 M 4-Br-C_6H_4-*t*-Bu, 0.200−0.563 M $NaOC(Et)_3$, and 20 mM aniline. Plots of the concentration of aniline versus time were not linear, again suggesting the possibility that aniline is involved in the rate-determining step of the catalytic cycle (Figure 6, top). In contrast, the decay of amine was linear for reactions containing concentrations of DPPF ranging from 17.9 to 80.2 mM (Figure 6, bottom). Under these conditions, the rate of the reaction was first order in aryl halide. The catalytic reaction showed no saturation of the observed rate constant at high [ArBr]. The reactions were inverse first order in DPPF in the concentration ranges indicated above and zero order in the alkoxide base.

Monitoring of the reaction of aniline with 4-Br-C_6H_4-*t*-Bu by $^{31}P\{^1H\}$ spectroscopy revealed why the decay of amine during reactions at low [DPPF] was nonlinear. The catalyst was gradually converted to the arylpalladium diarylamido complex (DPPF)Pd(4-C_6H_4-*t*-Bu)[N(Ph)(4-C_6H_4-*t*-Bu)] (**8**) and free DPPF, as determined by $^{31}P\{^1H\}$ NMR spectroscopy (Figure S7). Arylpalladium amido complexes of this class have been isolated and studied previously.[79] Complexes electronically similar to **8** undergo first-order reductive elimination at the higher temperature of 75 °C, with a half-life on the order of 10 min.[79] Thus,

(78) Uozumi, Y.; Suzuki, N.; Ogiwara, A.; Hayashi, T. *Tetrahedron* **1994**, *50*, 4293−4302.

(79) Driver, M. S.; Hartwig, J. F. *J. Am. Chem. Soc.* **1997**, *119*, 8232−8245.

the lifetime of this species in the catalytic system at 60 °C is similar to that of the DPPF-ligated Pd(0) species, and the presence of one or the other as a resting state depends on the concentration of product and the concentration of added DPPF. Early in the reaction, the concentration of diarylamine and, therefore, diarylamido complex are low. At high [DPPF], the rate of oxidative addition becomes slower than reductive elimination or exchange of the diarylamido ligand with aniline because of the inverse dependence of the oxidative addition k_{obs} on [ArBr]. The sole resting state becomes the Pd(0) complex **2**, and linear plots of the decay of aniline are observed at high [DPPF], as was shown in Figure 6.

Discussion

Resting State and (In)stability of ArBr Complexes. Amatore[50] and Ozawa[76] reported that the reduction of $Pd(OAc)_2$ in solutions containing triphenylphosphine[50] or BINAP[76] forms phosphine oxide and acetic anhydride. We observed no signals due to the monophosphine oxide of either DPPF or BINAP when $Pd(OAc)_2$ was used as a catalyst precursor,[75] and phosphine-ligated Pd(0) forms more rapidly in the presence of amine and base than in their absence. $^{31}P\{^1H\}$ NMR spectroscopy of reactions containing less than 2 equiv of ligand per palladium showed a single phosphine complex as the resting state. In such cases, a catalytically inactive, but soluble, phosphine-free palladium complex may exist, or the remaining palladium may simply precipitate from solution.[80]

The identity of the resting state depended on the phosphine ligand and type of amine substrate. Although not all of the pathways for decomposition of catalysts were determined, the BINAP-ligated palladium complex was unstable during reactions of secondary amines. The decomposition of the BINAP-ligated palladium catalyst is consistent with a lower reactivity of this catalyst toward secondary amines than toward primary amines. It is also consistent with the need for higher catalyst loadings with this class of substrate.[48] Similarly, the DPPF-ligated palladium(0) resting state was partially converted to an unproductive arylpalladium(II) diarylamido resting state. The observation of the arylpalladium diarylamido complex **8** is consistent with the competing formation of triarylamines during the reaction of anilines with unhindered aryl halides. The accumulation of **8** as resting state occurs because the rate for reductive elimination of triarylamine from **8** is similar to the qualitatively determined rate of oxidative addition of bromobenzene to **2**.

Irreversible cleavage of the backbone P−C bonds in BINAP and DPPF ligands is unusual. This cleavage process is more rapid for (BINAP)Pd(Ph)Br than for (DPPF)Pd(Ph)Br. The cleavage reaction for both compounds was slower than the reactions of the arylpalladium halides with primary amines during catalytic reactions, but it may account for some of the catalyst decomposition during reactions of secondary amines catalyzed by BINAP-ligated palladium. Moreover, this cleavage process may be an important catalyst decomposition pathway for other palladium-catalyzed processes that involve an arylpalladium halide resting state, particularly when polar solvents are used. For example, olefin insertion is often rate determining in Heck reactions,[81] transmetalation is often rate determining in Stille or Suzuki reactions,[82−85] and transmetalation or reductive elimination is likely to be rate determining in alcohol[77,86−89] and azole arylation.[64,90] The C−C bond-forming processes are often run in DMF or other polar solvents. In many of these reactions, BINAP has been used as a ligand for enantioselection or simply as an effective supporting ligand.[16,22−30] Thus, backbone P−C bond cleavage may lead to a change in catalyst structure for these processes when a chelating phosphine is used.

Scheme 3

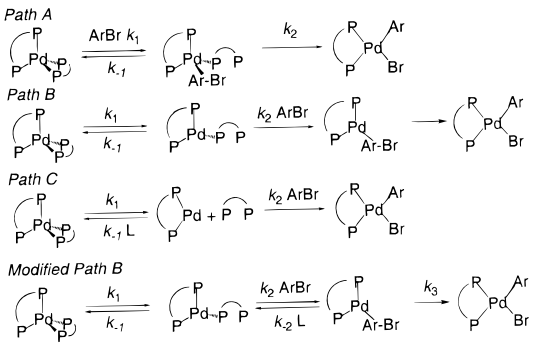

Mechanism of Aryl Halide Oxidative Addition to Pd(BINAP)$_2$ and Pd(DPPF)$_2$. Potential mechanisms for the oxidative addition of aryl bromides to $Pd(chelate)_2$ (chelate = DPPF, BINAP) are shown in Scheme 3. Path A involves the associative displacement of an arm of the chelating ligand with aryl bromide, followed by carbon−halogen bond cleavage by the 18-electron Pd(0) complex containing intact, coordinated aryl bromide. The rate law in eq 1 for this mechanism predicts a reaction that is first order in aryl bromide and zero order in added ligand.

Path A:

$$k_{obs} = \frac{k_1 k_2 [ArBr]}{k_{-1} + k_2} \qquad (1)$$

Path B involves reversible dissociation of an arm of the bisphosphine ligand, followed by irreversible associative displacement of the monocoordinated ligand, or irreversible carbon−halogen bond cleavage by the 16-electron species. The rate law for path B (eq 2) predicts that k_{obs} will, again, show a zero-order dependence on free ligand concentration.

Path B:

$$k_{obs} = \frac{k_1 k_2 [ArBr]}{k_{-1} + k_2 [ArBr]} \qquad \frac{1}{k_{obs}} = \frac{1}{k_1} + \frac{k_{-1}}{k_1 k_2 [ArBr]} \qquad (2)$$

Path B may, however, show a dependence of reaction rate on aryl bromide concentration that varies with [ArBr]. It is possible that zero-order behavior would be observed at high aryl bromide concentrations if k_2[ArBr] becomes significantly larger than k_{-1}. A variant of path B involving reversible coordination of aryl

(80) The precipitation of Pd(0) is difficult to observe unambiguously because of the formation of alkali halide salts during the amination reactions. "Ligandless" palladium, such as $Pd(OAc)_2$, $Pd(DBA)_2$, or (η-Cp)Pd(η-Allyl), does not catalyze the aryl halide amination reaction.

(81) van Strijdonck, G. P. F.; Boele, M. D. K.; Kammer, P. C. J.; de Vries, J. G. V.; van Leeuwen, P. W. N. M. *Eur. J. Inorg. Chem.* **1999**, 1073−1076.

(82) Farina, V.; Krishnan, B. *J. Am. Chem. Soc.* **1991**, *113*, 9585−9595.

(83) Farina, V.; Kapadia, S.; Krishnan, B.; Chenjie, W.; Liebeskind, L. S. *J. Org. Chem.* **1994**, *59*, 5905−5911.

(84) Farina, V. *Pure Appl. Chem.* **1996**, *68*, 73−78.

(85) Louie, J.; Hartwig, J. F. *J. Am. Chem. Soc.* **1995**, *117*, 11598.

(86) Mann, G.; Hartwig, J. F. *Tetrahedron Lett.* **1997**, *38*, 8005.

(87) Mann, G.; Hartwig, J. F. *J. Org. Chem.* **1997**, *62*, 5413.

(88) Mann, G.; Incarvito, C.; Rheingold, A. L.; Hartwig, J. F. *J. Am. Chem. Soc.* **1999**, *121*, 3224.

(89) Aranyos, A.; Old, D. W.; Kiyomori, A.; Wolfe, J. P.; Sadighi, J. P.; Buchwald, S. L. *J. Am. Chem. Soc.* **1999**, *121*, 4369−4378.

(90) Mann, G.; Hartwig, J. F.; Driver, M. S.; Fernandez-Rivas, C. *J. Am. Chem. Soc.* **1998**, *120*, 827.

bromide will be discussed below. Path C involves the full dissociation of a chelating ligand and direct oxidative addition of the aryl bromide to the 14-electron intermediate. The rate law for path C (eq 3) predicts different reaction orders at different ratios of aryl bromide to free ligand.

Path C:

$$k_{obs} = \frac{k_1 k_2 [ArBr]}{k_{-1}[L] + k_2[ArBr]} \qquad \frac{1}{k_{obs}} = \frac{1}{k_1} + \frac{k_{-1}[L]}{k_1 k_2 [ArBr]} \quad (3)$$

$$k_{obs} = \frac{k_1 k_2 [ArBr]}{k_{-1}[L] + k_2[ArBr]} = k_1 \qquad \text{when } [ArBr] \gg [L] \quad (4)$$

Depending on the ratio of rate constants k_2 and k_{-1}, the reaction can be first order in aryl bromide and inverse first order in free ligand when the ratio [ArBr]:[L] is small, but zero order in both when [ArBr]:[L] is large. When [ArBr] is high, the rate law simplifies to that shown in eq 4. The unsaturated intermediates in pathways B and C can exist with solvent directly coordinated to the Pd(0) species or with no direct interaction of the intermediate with a discrete solvent molecule.

Our data rule out paths A and B for the oxidative addition reactions. Path A is inconsistent with the zero-order rate behavior at high [ArBr]. Both path A and path B are inconsistent with the inverse dependence of k_{obs} on ligand concentration. Of paths A−C, only path C is consistent with a first-order dependence on [PhBr] at low concentrations, a zero-order dependence on [PhBr] at high concentrations of aryl bromide, and an inverse first-order dependence on [BINAP] when the aryl bromide concentration is low.

We cannot, however, distinguish between path C and the variant of path B in Scheme 3. This modified mechanism involves reversible displacement of the ligand by aryl bromide through a combination of dissociative and associative steps to generate a Pd(0) complex (BINAP)Pd(ArBr) containing intact aryl bromide. The rate law in eq 5 for this mechanism, which contains its two preequilibria, is complex but predicts reaction orders similar to those in path C.

Modified Path B:

$$k_{obs} = \frac{k_1 k_2 k_3 [ArBr]}{k_{-1}k_3 + k_{-1}k_{-2}[L] + k_2 k_3 [ArBr]}$$

$$\frac{1}{k_{obs}} = \frac{1}{k_1} + \frac{k_{-1}}{k_1 k_2 [ArBr]} + \frac{k_{-1}k_{-2}[L]}{k_1 k_2 k_3 [ArBr]} \quad (5)$$

$$k_{obs} = \frac{k_1 k_2 k_3 [ArBr]}{k_{-1}k_3 + k_{-1}k_{-2}[L] + k_2 k_3 [ArBr]} = k_1$$

$$\text{when } [ArBr] \gg [L] \quad (6)$$

This rate equation simplifies to that in eq 6 if [ArBr] is high, as does the rate law for path C. These rate equations are similar because the oxidative addition occurs to an intermediate coordinated by a single bis-phosphine ligand in both cases. Thus, our data demonstrate that carbon−halogen bond cleavage occurs either directly by (BINAP)Pd or after coordination to palladium and formation of (BINAP)Pd(ArBr), which contains coordinated, intact aryl bromide. We favor path C over this modified path B. Saturation of k_{obs} at high [PhBr] requires that the [(κ^1-BINAP)(κ^2-BINAP)Pd(0)] coordinates PhBr as a dative ligand much faster than it recoordinates the arm of the κ^1-BINAP. This requirement seems unreasonable, considering the intermolecularity of the PhBr coordination and the weak donating ability of PhBr.

Scheme 4

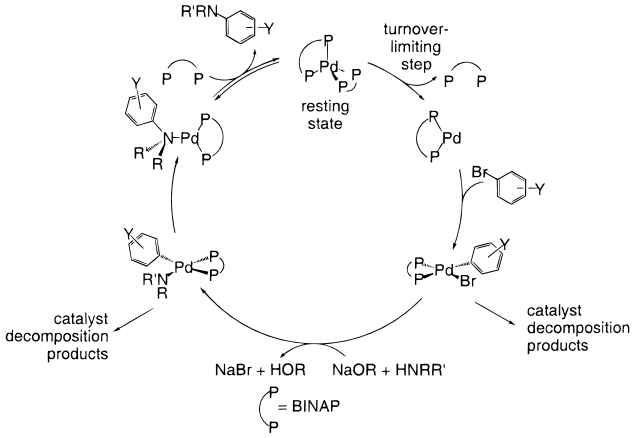

Scheme 5

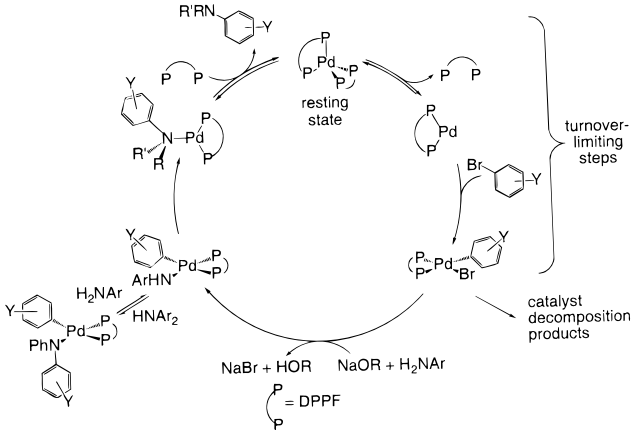

Our observation that the rate of the oxidative addition is independent of the identity and coordinating ability of the solvent suggests that a discrete solvent molecule is not directly coordinated to the Pd(0) intermediate that adds aryl bromide. Pd(0) amine complexes are not observed in these reactions. Although amine may coordinate reversibly to the unsaturated Pd(0) intermediate, the lack of rate dependence on the presence or absence of amine demonstrates that an amine complex is not an intermediate for addition of aryl bromides.

Although we did not obtain quantitative rate data for the oxidative addition of aryl bromide to DPPF complex **2** because of the difficulty in isolating pure **2**, we did observe a clear inverse dependence of k_{obs} on the concentration of free DPPF. Thus, $Pd(DPPF)_2$ also undergoes oxidative addition by a mechanism involving an intermediate containing a single bis-phosphine ligand formed by full dissociation of a coordinated DPPF.

Kinetic Studies of the Reaction of Amines with Aryl Bromides Catalyzed by $Pd(BINAP)_2$ and $Pd(DPPF)_2$. A summary of the mechanistic conclusions for the reactions of primary amines catalyzed by BINAP complex **1a** is provided in Scheme 4, and a summary of our conclusions for reactions of aniline catalyzed by DPPF-ligated palladium is provided in Scheme 5. As expected, our data are consistent with the general mechanism involving oxidative addition of aryl halide, generation of an amido intermediate from amine and base, and reductive elimination to form product. However, the zero-order rates at high ArBr for reactions catalyzed by **1a** require that the reaction scheme be different from that shown in Scheme 6 proposed previously.[91,92] The different rate behavior for reactions

Scheme 6

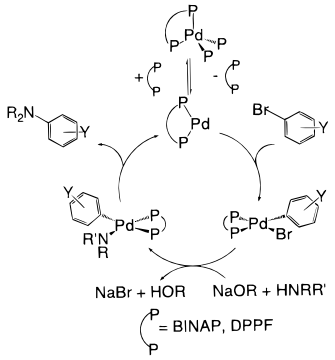

of secondary amines catalyzed by **1a** and the nonlinear plots for the decay of amine for reactions catalyzed by **2** require changes in the catalyst during the reaction.

If the Pd(0) species is the resting state and oxidative addition of aryl halide is irreversible, then oxidative addition would be the turnover-limiting step. Our studies on the mechanism of oxidative addition to **1a** showed that ligand dissociation was irreversible and rate limiting when the ratio of [ArBr]:[L] was high, as it is in the catalytic reactions. Thus, the rate of the oxidative addition process and the rate of the catalytic cycle depend only on the rate of dissociation of BINAP from **1a**, as shown in Scheme 4. In this case, the observed zero-order rate constant for the catalytic reaction, shown in eq 7, is the product of the catalyst concentration and the observed rate constant for the oxidative addition of PhBr to **1a** at 60 °C. This calculated rate constant is within a factor of 3 of the measured rate constant for the reaction of primary amines with aryl halide catalyzed by **1a**.

$$k_{obs} = \frac{k_1 k_2 [ArBr][PdL_2]}{k_{-1}[L] + k_2[ArBr]} = k_1[PdL_2] \qquad \text{when } [ArBr] \gg [L] \tag{7}$$

In the previously proposed mechanism of Scheme 6, **1a** does not lie on the catalytic cycle. It generates the actual catalyst by a preequilibrium of phosphine dissociation. This mechanism is inconsistent with the zero-order rate behavior at high [PhBr]. The number of turnovers for each (BINAP)Pd(0) generated would depend on the relative concentrations of [PhBr] and [BINAP]. For example, the intermediate (BINAP)Pd(0) would be more likely to add PhBr to initiate a second turnover when the ratio of PhBr:BINAP is high; it would be more likely to re-form the resting state **1a** when the ratio of PhBr:BINAP is low. Kinetic simulations using rate constant information from the oxidative addition process showed that the rates for reactions by the mechanism in Scheme 6 would depend on [ArBr] and [BINAP]. To observe the same rate behavior for the stoichiometric oxidative addition and catalytic reactions, the species involved in the oxidative addition mechanism must be an intermediate in the catalytic cycle. A single ligand dissociation event must lead to formation of a single product molecule. Thus, the mechanisms in Schemes 4 and 5 are consistent with our data.

In the mechanism of Scheme 4, **1a** lies on the reaction path and (BINAP)Pd is an intermediate in the oxidative addition. If reductive elimination involves this same intermediate, the process in Scheme 6 would result. Thus, reductive elimination cannot involve free (BINAP)Pd. We suggest that reductive elimination irreversibly forms a 16-electron amine-ligated Pd(0), which reacts with BINAP in an associative step to form **1a**. The oxidative addition could also occur by formation of an ArBr complex by modified path B, but we disfavor this reaction mechanism as discussed above. Scheme 4, therefore, involves closely related but distinct pathways for oxidative addition of aryl halide and reductive elimination of amine.

For reactions of aniline with aryl bromides catalyzed by **2**, the saturation of the rate constant for oxidative addition at high [ArBr] was not observed as it was for reactions of **1a**. Thus, recoordination of DPPF was always faster than oxidative addition of aryl bromide. A first-order dependence of k_{obs} on aryl bromide concentration and an inverse first-order dependence of k_{obs} on ligand concentration were, therefore, observed. The observation of **2** as the resting state when DPPF was added to the reaction predicts the same rate behavior for the catalytic reactions and the stoichiometric oxidative addition. This result was observed, supporting a catalytic mechanism in which the combination of ligand dissociation and irreversible cleavage of the carbon−halogen bond control the rate of the catalytic process. Considering the similarity in ligand structures, we suggest that DPPF-ligated **2** catalyzes the arylation of anilines by the same path as does **1a**, but the C−X cleavage step is never fast enough relative to recoordination of ligand to give saturation in [ArBr].

Effect of Catalyst Changes during the Aminations. Two additional sets of unexpected rate data were obtained, one for reactions of secondary amines with aryl bromides catalyzed by **1a**, and one for reactions of anilines with aryl bromides catalyzed by **2** at low concentrations of added DPPF. These two reactions underscore the importance of clearly determining the catalyst resting state when interpreting the kinetic data on a catalytic system.

One set of data appeared to show a first-order decay of amine for the reactions of secondary amines with aryl bromides catalyzed by **1a**. In the absence of data on the resting state, one might conclude that the reaction rate was first order in amine and that reactions of secondary amines involved a resting state, such as an arylpalladium halide complex, that reacts with amine. Instead, the observation of catalyst decomposition and the confirmation that all stoichiometric reactions after oxidative addition are faster than the oxidative addition demonstrated that the unexpected decay was due to decomposition of the catalyst (Figure S6) in a reaction that depends only on catalyst concentration. One catalyst decomposition path is backbone P−C bond cleavage. The palladium binaphthylmonophosphine complex that would result is much less active for amination than the BINAP-palladium complexes.[92]

The second set of data could also have been interpreted as a change in turnover-limiting step for the reaction of aniline with aryl bromides catalyzed by **2**. However, this behavior was again due to a reduction in the concentration of active catalyst. Unlike the irreversible formation of inactive species during the reactions of secondary amines catalyzed by **1a**, catalyst **2** was reversibly converted to the arylpalladium diarylamido complex **8** by reaction with product.

The final unexpected observation is the slightly slower reaction of aniline with aryl halides catalyzed by **1a** than we observed with other amines. The plots of the decay of amine with time were linear as expected, but the rate of reaction was roughly 25% slower than that for reactions of the other amines. In this case, only 15% decomposition of the catalyst was observed during the reaction. The observed rate constant was

(91) Hartwig, J. F. *Angew. Chem., Int. Ed.* **1998**, *37*, 2046−2067.
(92) Wolfe, J. P.; Buchwald, S. L. *J. Org. Chem.* **2000**, *65*, 1144−1157.

reproducible and independent of the purity of the aniline used. We do not have an explanation for this single observation.

Comparison to the Kinetic Behavior of Other Catalytic Systems. Few transition metal-catalyzed reactions are zero order in all reagents. This kinetic situation must result from a unimolecular reaction of the catalyst. Ligand dissociation, reductive elimination, and intramolecular insertion are examples of such unimolecular reactions. The previously reported zero-order reactions include those with turnover-limiting olefin or CO insertion into M−X bonds, as in certain hydroamination/cyclization reactions,[93,94] Heck reactions,[81,95] hydroformylations,[96] and alkyne isomerizations.[97,98] Except for cyclizations, these cases typically involve rate measurements using excess quantities of a reagent which does display a reaction order; these reactions are, therefore, pseudo zero order and are different from the case reported here for reactions catalyzed by **1a** that are zero order in all reagents due to saturation behavior. Lanthanide-catalyzed hydroamination/cyclization is truly zero order in all reagents. This observation results from the intramolecularity of the turnover-limiting insertion reaction. In contrast to organometallic catalysts, many enzymes show zero-order rate behavior. In these biological systems, zero-order behavior results from rate-limiting product release.[99] One can envision that transition metal Lewis acid catalysts could also show such rate-limiting product release.

Summary and Conclusions

We have shown that the rate of oxidative addition and the stability of the catalyst toward decomposition and product inhibition dictate the kinetic behavior of the catalytic cycle and that bis-chelate complexes **1a** and **2** are likely to lie on the actual catalytic cycles. We have also shown that results from examining the catalyst stability by ^{31}P NMR spectroscopy throughout the reaction explain unexpected deviations from the predicted rate behavior. Although not all pathways leading to catalyst decomposition and inactivation have been identified, some of the most significant ones were detected. For reactions catalyzed by BINAP-ligated palladium, the thermal instability of the ligand and the removal of palladium as inactive complexes that do not contain phosphorus are important pathways for deactivation of the catalyst. For reactions containing DPPF as ligand, an additional pathway involving formation of a diarylamido complex, which is more stable than the monoarylamido complex, stores the palladium in an unproductive form. These results demonstrate the importance of carefully determining the catalyst resting state from data that are independent of the rate behavior and of obtaining quantitative rate behavior for the overall catalytic process.

Experimental Section

General Considerations. Unless otherwise noted, all manipulations were conducted using standard Schlenk techniques or in an inert atmosphere glovebox. ^{1}H NMR spectra were obtained on Bruker AM 500-MHz, GE QE 300-MHz, GE Ω 500-MHz, or GE Ω 300-MHz Fourier transform NMR spectrometers. ^{31}P{^{1}H} NMR spectra were obtained on the Ω 300- and 500-MHz spectrometers operating at the corresponding frequencies. ^{1}H NMR spectra were recorded relative to residual protiated solvent. ^{31}P{^{1}H} NMR spectra were recorded in units of parts per million relative to 85% H_3PO_4 as external standard. UV−visible spectra were collected on a Varian Cary 3E spectrophotometer equipped with a thermostated multicell block.

Unless specified otherwise, all reagents were purchased from commercial suppliers and used without further purification. Pd[P(*o*-Tol)$_3$]$_2$,[100] Pd(DBA)$_2$, (PPh$_3$)$_2$Pd(Ph)Br,[101] (DPPF)Pd(Ph)Br,[79] and (DPPF)Pd(4-C$_6$H$_4$-*t*-Bu)Br[100] were prepared using literature procedures, unless otherwise noted. Protiated solvents were heated to reflux and distilled from purple solutions containing sodium benzophenone ketyl. Deuterated solvents were dried similarly but were collected by vacuum transfer. Dichloromethane and dichloromethane-d_2 were dried over CaH_2 and distilled or vacuum transferred, respectively.

Preparation of Pd(BINAP)$_2$ (1a). Into a 20-mL screw-capped vial were weighed Pd[P(*o*-Tol)$_3$]$_2$ (102.3 mg, 0.143 mmol) and BINAP (180.1 mg, 0.289 mmol), followed by 3 mL of benzene. The dark red reaction mixture was filtered through Celite, layered with pentane, and allowed to stand at room temperature for 5 h. Red crystalline solid was collected by filtration and dried in vacuo to give 173.7 mg (89.7%) of Pd(BINAP)$_2$. ^{1}H NMR (500 MHz C$_6$D$_6$): δ 5.87 (t, J = 7.6 Hz, 8H), 6.18 (t, J = 7.4 Hz, 4H), 6.84 (app t, J = 7.7 Hz, 4H), 7.05 (app t, J = 7.3 Hz, 4H), 7.14−7.26 (m, 16H), 7.33−7.39 (m, 8H), 7.47 (broad, 8H), 7.82 (broad m, 4H), 8.36 (broad, 8H). ^{31}P{^{1}H} NMR (C$_6$D$_6$): δ 27.4 (s).

Preparation of Pd((*R*)-Tol-BINAP)$_2$ (1b). Into a 20-mL screw-capped vial were weighed Pd[P(*o*-Tol)$_3$]$_2$ (152 mg, 0.212 mmol) and (*R*)-Tol-BINAP (289 mg, 0.439 mmol), followed by 5 mL of benzene. The dark red reaction mixture was filtered through Celite, layered with pentane, and allowed to stand at room temperature for 5 h. Dark red crystals suitable for X-ray diffraction were collected by careful mechanical removal from the reaction medium (100 mg). An additional 107 mg of microcrystalline solid was collected by filtration and drying in vacuo of the additional solid left after removal of the large crystals. These two crops yielded a total of 207 mg (66.8%) of Pd((*R*)-Tol-BINAP)$_2$. ^{1}H NMR (500 MHz C$_6$D$_6$): δ 1.52 (s, 12H), 2.11 (s, 12H), 5.77 (d, J = 8.1 Hz, 8H), 6.82−6.95 (m, 8H), 7.00−7.10 (m, 4H), 7.19 (d, J = 7.5 Hz, 8H), 7.31 (d, J = 8.4 Hz, 4H), 7.38 (d, J = 8.0 Hz, 4H), 7.49 (broad, 8H), 8.03 (broad m, 4H), 8.39 (broad, 8H). ^{31}P{^{1}H} NMR (C$_6$D$_6$): δ 24.60 (s). Anal. Calcd for C$_{96}$H$_{80}$P$_4$Pd: C, 78.76; H, 5.51 Found: C, 78.60; H, 5.65.

Preparation of Pd(DPPF)$_2$ (2). Into a 20-mL screw-capped vial were weighed Pd[P(*o*-Tol)$_3$]$_2$ (101.2 mg, 0.142 mmol) and DPPF (156.5 mg, 0.282 mmol), followed by 5 mL of benzene. The orange-yellow reaction mixture was filtered through Celite and layered with 10 mL of pentane. Yellow powder (119.8 mg) was collected by filtration and dried in vacuo. This material consisted of a mixture of Pd(DPPF)$_2$, [Pd(DPPF)]$_2$(μ-DPPF)], and free DPPF, as determined by ^{31}P and ^{1}H NMR spectroscopy. ^{1}H NMR (300 MHz C$_6$D$_6$): δ 4.00 (s, 8H), 4.29 (s, 8H), 6.8−7.05 (m, 24H), 7.78 (broad, 16 H). ^{31}P{^{1}H} NMR (C$_6$D$_6$): δ 7.73 (s).

Isolation of [Pd(DPPF)]$_2$(μ-DPPF) (3). A freshly prepared batch of impure Pd(DPPF)$_2$ (40.0 mg, 32.9 μmol) was redissolved in approximately 15 mL of THF. The resulting solution was cooled to −34 °C and then layered with approximately 5 mL of ether and returned to the freezer at −34 °C, where it was left standing for 48 h. Crystals suitable for X-ray diffraction were collected by decanting the solvent from the reaction vessel and examining the crystalline material visually.

Preparation of {Pd[P(*o*-Tol)$_3$](Ph)(μ-Br)}$_2$ (7). Pd[P(*o*-Tol)$_3$]$_2$ (105.2 mg, 0.147 mmol) was added to a solution of bromobenzene (114.6 mg, 0.730 mmol) in 25 mL of benzene with stirring. After reaction at ambient temperature for 30 min, the resulting pale yellow solution was filtered through a bed of Celite to remove any insoluble material. The clear yellow solution was allowed to react at room temperature for an additional 5 h and was then concentrated in vacuo to 1/10 of the original volume. The resulting suspension was layered

(93) Arredondo, V. M.; McDonald, F. E.; Marks, T. J. *J. Am. Chem. Soc.* **1998**, *120*, 4871−4872.
(94) Li, Y.; Marks, T. J. *J. Am. Chem. Soc.* **1998**, *120*, 1757−1771.
(95) Beller, M.; Riermeier, T. H. *Eur. J. Inorg. Chem.* **1998**, *1*, 29−35.
(96) Vrieze, K.; Groen, J. H.; Delis, J. G. P.; Elsevier: C. J.; van Leeuwen, P. W. N. M. *New. J. Chem.* **1997**, *21*, 807−813.
(97) Coolen, H. K. A. C.; Nolte, R. J. M.; van Leeuwen, P. W. N. M. *J. Organomet. Chem.* **1995**, *496*, 159−168.
(98) Salomon, R. G.; Salomon, M. F.; Kachinski, J. L. *J. Am. Chem. Soc.* **1977**, *94*, 1043−1054.
(99) Walsh, C. *Ezymatic Reaction Mechanisms*; W. H. Freeman and Co.: New York, 1979.
(100) Paul, F.; Patt, J.; Hartwig, J. F. *Organometallics* **1995**, *14*, 3030.
(101) Fitton, P.; Johnson, M. P.; McKeon, J. E. *J. Chem. Soc., Chem. Commun.* **1968**, 6−7.

with ether and allowed to stand at ambient temperature for 5 h to yield 58.5 mg (70.0%) of an insoluble pale yellow powder. Anal. Calcd for $C_{54}H_{52}Pd_2Br_2P_2$: C, 57.12; H, 4.62. Found: C, 57.38; H, 4.83.

Preparation of (*rac*-BINAP)Pd(Ph)(Br) (5). Pd[P(*o*-Tol)$_3$]$_2$ (1.010 g, 1.41 mmol) was added to a solution of bromobenzene (1.18 g, 7.54 mmol) in 120 mL of benzene with stirring. After reaction at ambient temperature for 30 min, the resulting pale yellow solution was filtered through a bed of Celite to remove any insoluble material. The resulting clear yellow solution was then allowed to react at room temperature for approximately 5 h. After this time, racemic BINAP (877.8 mg, 1.41 mmol) was added, and the reaction was continued until all solid material dissolved. The final solution was then concentrated to 1/10 of the original volume in vacuo and layered with ether. A pale yellow powder was obtained. After recrystallization by layering a concentrated solution of the product in CH_2Cl_2 with ether, 637.9 mg of pale yellow microcrystals with the formula (BINAP)Pd(Ph)Br·$^1/_2CH_2Cl_2$ was obtained in 50.0% yield. ^{1}H NMR (300 MHz, C_6D_6): δ 5.33 (s, 1H, CH_2Cl_2 of crystallization), 6.21 (m, 2H), 6.36 (m, 4H), 6.57 (m, 2H), 6.68−7.32 (m, 16H), 7.48 (app d, 2H), 7.60 (broad, 2H), 7.82 (app t, 2H), 7.98 (app t, 3H), 8.08 (app t, 4H). ^{31}P{^{1}H} NMR: δ 28.21 (d, J_{PP} = 39.06 Hz), 11.78 (d, J_{PP} = 39.07 Hz). Anal. Calcd for $C_{50}H_{37}P_2PdBr\cdot{}^1/_2CH_2Cl_2$: C, 65.32; H, 4.12. Found: C, 65.32; H, 4.63.

Thermolysis of (DPPF)Pd(Ph)Br and (BINAP)Pd(Ph)Br. A solution of (DPPF)Pd(Ph)Br (5.0 mg, 6.1 μmol) or (BINAP)Pd(Ph)Br (5 mg, 5.6 μmol) in THF, benzene, or toluene was transferred to a screw-capped NMR tube. The solution of (BINAP)Pd(Ph)Br was heated at 70 °C for 14 h. The solution of (DPPF)Pd(Ph)Br was heated at 110 °C for 16 h. The reaction was monitored by ^{31}P{^{1}H} or ^{1}H spectroscopy in the case of (DPPF)Pd(Ph)Br at several intervals before the reaction was complete. After this time, addition of 2.5 equiv of diphenylmethylphosphine to the reaction mixture produced a new set of doublets and a resonance corresponding to that of free PPh_3.

Preparation of *rac*-(PPh_3)(Br)Pd[2′-(diphenylphosphino)-2-yl-(1,1′-binaphthyl)] (6). A 250-mL reaction vessel fused to a Kontes vacuum adapter was charged with (*rac*-BINAP)Pd(Ph)Br (1.420 g, 1.60 mmol) and 180 mL of benzene. The solution was heated at 65 °C for 14 h. The reaction was evaporated to dryness, and the residue was redissolved in 10 mL of benzene. The resulting solution was layered with pentane, and after several hours, 1.25 g (88.3%) of crystalline product was isolated by filtration. This material contained half a molecule of benzene per molecule of product. Crystals suitable for X-ray diffraction were manually selected from this sample. ^{1}H NMR (C_6D_6): δ 6.44 (broad, 1H), 6.51 (m, 1H), 6.79 (m, 2H), 6.86 (m, 8H), 6.9−6.96 (m, 2H), 7.01−7.25 (m, 10H), 7.36 (dd, J_1= 8.49 Hz, J_2 = 7.08 Hz, 1H), 7.44 (dd, J_1 =7.39, J_2 = 8.55, 1H), 7.49 (d, broad, 1H), 7.54 (d, broad, 1H), 7.60 (d, broad, 1H), 7.70−7.76 (m, 6H), 8.04 (app t, J = 9.21 Hz). ^{31}P{^{1}H} NMR (C_6D_6): δ 31.3 d, 23.6 d (J_{PP} = 440 Hz) (relative peak heights, outer to inner, 35:100). Anal. Calcd for $C_{50}H_{37}P_2PdBr\cdot{}^1/_2C_6H_6$: C, 68.81; H, 4.36. Found: C, 68.47; H, 4.34.

Oxidative Addition of PhBr to Pd(chelate)$_2$ (chelate = BINAP or DPPF) and Qualitative Observation of Reaction Orders. Pd(chelate)$_2$ (1.8−2.2 μmol), ligand (BINAP or DPPF; 1.8−25 μmol), and 1,3,5-trimethoxybenzene or ferrocene as internal standard were dissolved in 0.5 mL of benzene-d_6 and transferred to a screw-capped NMR tube containing a PTFE-lined septum cap. PhBr (1−100 μL, 9−900 μmol) was added via syringe to this solution. An initial ^{1}H NMR spectrum was acquired, and the mixture was heated at 55−85 °C. ^{1}H NMR spectroscopic data were collected at various reaction times, and a yield was determined by comparing the integrals of product resonances and internal standard in the final spectrum vs those of starting material and standard in the initial spectrum.

Determination of the Oxidative Addition Rate of PhBr to Pd(BINAP)$_2$. Separate stock solutions of Pd(BINAP)$_2$, BINAP, and PhBr were prepared by dissolving Pd(BINAP)$_2$, BINAP, and PhBr in benzene. Similar stock solutions were prepared in THF and 2,5-dimethyl-THF. The stock solutions were stored in at −35 °C in a freezer. For experiments to determine the reaction order in BINAP, the PhBr concentration was fixed at 1.78×10^{-3} M, the Pd(BINAP)$_2$ concentration was either 7.10×10^{-6} or 3.05×10^{-5} M to obtain reasonable reaction times, and the concentration of BINAP was varied between 3.60×10^{-5} and 2.98×10^{-4} M. For experiments to determine the reaction order in PhBr, [Pd(BINAP)$_2$] and [BINAP] were held constant at 2.26×10^{-5} and 1.08×10^{-4} M respectively, and [PhBr] was varied from 1.78×10^{-3} to 8.95×10^{-2} M. For the determination of the rate of oxidative addition of ortho-substituted aryl bromides, [Pd(BINAP)$_2$] and [BINAP] were held constant at 2.26×10^{-5} and 1.08×10^{-4} M, respectively, and neat aryl bromide was added to the reaction to obtain an aryl bromide concentration of 8.95×10^{-2} M. For the determination of solvent and additive effects, the concentrations of Pd(BINAP)$_2$, BINAP, and PhBr were fixed at 2.29×10^{-5}, 1.72×10^{-4}, and 1.84×10^{-3}, respectively. Samples were prepared by adding stock solutions into a 5-mL volumetric flask. Each flask was then filled to the 5-mL volumetric mark with the appropriate solvent. The resulting solutions were shaken and transferred (∼3 mL) to quartz cuvettes fitted with an airtight Teflon valve. The UV−visible spectrometer cell block was warmed to 45 °C. The absorbance of Pd(BINAP)$_2$ was monitored at λ = 519 nm, with a 1-s signal averaging time, and 30 s between acquisitions over at least three half-lives. Kinetic data were fit to the expression $A_{519} = B\ e^{kt} + c$, in which k is the pseudo-first-order rate constant k_{obs}.

Rate Determination of Amination of Bromobenzene with Primary Amines Using Pd(BINAP)$_2$ as Catalyst. A stock solution consisting of 3.75 mM Pd(BINAP)$_2$, 3.87 mM BINAP, 408.9 mM NaOC(Et)$_3$, and an internal standard (ferrocene or 1,3,5-trimethoxybenzene) was prepared in benzene-d_6 and stored in a −35 °C freezer. Another stock solution was prepared containing a 4.80 M concentration of bromobenzene in C_6D_6. A typical reaction mixture was prepared by mixing 0.200 mL of the first stock solution with 0.150 mL of the second and 0.250 mL of C_6D_6 in a screw-capped NMR tube. Neat reagents were added to the reaction mixture to obtain higher concentrations of bromobenzene, ligand, or base. The total volume was maintained constant at 0.600 mL by appropriately reducing the amount of additional C_6D_6 added to the reaction. Amines were injected into the NMR tube via syringe immediately prior to the initiation of the data acquisition program. Volumes of amine injected were varied so that initial oncentration of amine would be 12.6 mM (typically 0.6−1.2 μL). Amines were used as received without prior drying or degassing, with the exception of aniline which was used as received and also after purification by distillation under nitrogen over activated molecular sieves. Zero-order rate constants were obtained by fitting a linear plot of the amine starting material concentration versus time to the expression $y = mx + b$, in which m is the zero-order rate constant k_{obs}.

Rate Determination of Amination of Bromobenzene with Aniline Using Pd(DPPF)$_2$ as Catalyst. A stock solution consisting of 8.0 mM (DPPF)Pd(4-C_6H_4-*t*-Bu)(Br), 16.0 mM DPPF, 4.800 M 4-bromo-*tert*-butylbenzene, and an internal standard (1,3,5-trimethoxybenzene) was prepared in benzene-d_6 and stored in a −35 °C freezer. Another stock solution was prepared containing 0.800 M NaOC(Et)$_3$ in C_6D_6. A typical reaction mixture was prepared by mixing 0.150 mL of the first stock solution with 0.150 mL of the second, and 0.300 mL of C_6D_6 in a screw-capped NMR tube. Neat reagents were added to the reaction mixture to obtain higher concentrations of bromobenzene, ligand, or base. The total volume was maintained at 0.600 mL by appropriately reducing the amount of additional C_6D_6 added to the reaction. Aniline was injected into the NMR tube via syringe immediately prior to the initiation of the data acquisition program. Zero-order rate constants were obtained by fitting a plot of the amine starting material versus time to the expression $y = mx + b$, where m is the zero-order rate constant k_{obs}. The initial linear portion of a plot was used whenever product inhibition prevented the use of the entire time course.

Determination of the Resting State in Reactions Catalyzed by 1a. Pd(BINAP)$_2$ (5.0 mg, 3.7 μmol), 4-bromotoluene (6.3 mg, 37 μmol), and NaO-*t*-Bu (4.3 mg, 44 μmol) were dissolved in 0.5 mL of benzene and transferred to a screw-capped NMR tube. Butylamine (4 μL, 40 μmol) was added via syringe. The tube was then placed into the NMR spectrometer probe and heated at 75 °C. ^{31}P{^{1}H} NMR spectra were obtained during the course of the reaction until the bromoarene was judged completely consumed by GC/MS.

Determination of the Resting State in the Amination of Aniline Catalyzed by Pd(OAc)$_2$ and BINAP. Pd(OAc)$_2$ (0.8 mg, 3.5 μmol), BINAP (4.6 mg 7.4 μmol), 4-bromotoluene (6.3 mg, from 37 μmol to 48 mmol), and NaO-*t*-Bu (4.3 mg, 44 μmol) were dissolved in 0.5 mL

of benzene and transferred to a screw-capped NMR tube. Butylamine (4 μL, 40 μmol) was added via syringe. The tube was then placed in the NMR spectrometer probe and heated at 75 °C. $^{31}P\{^1H\}$ NMR spectra were obtained during the course of the reaction, until the bromoarene was judged completely consumed by GC/MS. Two similar experiments were performed that contained 2.3 and 1.2 mg of BINAP.

Determination of the Resting State in the Amination of Aniline Catalyzed by 1a. $Pd(BINAP)_2$ (5 mg, 3.7 μmol), BINAP (2.3 mg, 3.7 μmol), bromobenzene (75.3 mg, 48 mmol), $NaOC(Et)_3$ (51.1 mg, 0.369 mmol), and tri-*o*-tolylphosphine (internal standard, 1.0 mg, 3.3 μmol) were dissolved in 0.550 mL of benzene-d_6 and transferred to a screw-capped NMR tube. Aniline (3.4 μL, 37 μmol) was added via syringe. The tube was then placed in the NMR spectrometer probe and heated at 60 °C. $^{31}P\{^1H\}$ NMR spectra were obtained during the course of the reaction until aniline was judged completely consumed by ^1H NMR spectroscopy.

Determination of the Resting State in the Amination of Secondary Amines Catalyzed by 1a. $Pd(BINAP)_2$ (5 mg, 3.7 μmol), BINAP (2.3 mg, 3.7 μmol), bromobenzene (75.3 mg, 0.480 mmol), and $NaOC(Et)_3$ (11.3 mg, 81.7 μmol) were dissolved in 0.550 mL of benzene-d_6 and transferred to a screw-capped NMR tube. *N*-Methylaniline (4.0 μL, 37 μmol) was added via syringe. The tube was then placed in the NMR spectrometer probe and heated at 60 °C. $^{31}P\{^1H\}$ NMR spectra were obtained during the course of the reaction until the *N*-methylaniline was judged completely consumed by ^1H NMR spectroscopy.

Determination of the Resting State in Reactions Catalyzed by 2. (DPPF)Pd(4-C_6H_4-*t*-Bu)(Br) (5.0 mg 6.1 μmol), DPPF (6.8 mg, 12.2 μmol), 4-bromo-*tert*-butylbenzene (83.2 μL, 0.480 mmol), $NaOC(Et)_3$ (84.3 mg, 0.610 mmol), and tri-*o*-tolylphosphine (internal standard 1.0 mg, 3.3 μmol) were dissolved in 0.515 mL of benzene-d_6 and transferred to a screw-capped NMR tube. Aniline (5.6 μL, 61 μmol) was added via syringe. The tube was then placed in the NMR spectrometer probe and heated at 60 °C. $^{31}P\{^1H\}$ NMR spectra were obtained during the course of the reaction until aniline was judged completely consumed by ^1H NMR spectroscopy.

Reductive Elimination of *N*-Phenylmorpholine from (BINAP)Pd(Ph)Br (5). A solution of **5** (5.0 mg, 5.6 μmol), BINAP (7.0 mg, 11.3 μmol), and ferrocene (internal standard) in 0.5 mL of benzene-d_6 was prepared and transferred to a screw-capped NMR tube containing a septum cap lined with PTFE. A ^1H NMR spectrum was obtained. This solution was then quickly transferred via syringe to another similar NMR tube containing lithium morpholide (0.6 mg, 6.5 μmol). The sample was quickly cooled to 0 °C in an ice bath and transferred to the NMR spectrometer probe at room temperature. Another ^1H NMR spectrum was obtained to determine the yield of *N*-phenylmorpholine. The same reaction was repeated by adding a solution of morpholine (1 μL, 11.4 μmol) and $NaOC(Et)_3$ (1.6 mg, 11.4 μmol) in benzene-d_6 (0.1 mL) to a similar solution of **5**, BINAP, and internal standard. The experiments were repeated in order to obtain $^{31}P\{^1H\}$ spectra. In all cases, greater than 95% yield of *N*-phenylmorpholine was observed immediately, and the only detectable palladium species observed by $^{31}P\{^1H\}$ NMR spectroscopy was **1a**.

X-ray Crystal Structure of Pd[(*R*)-Tol-BINAP]$_2$ (1b). A red platelike crystal of $C_{108}H_{92}P_4Pd$ having approximate dimensions of 0.20 × 0.41 × 0.45 mm^3 was mounted on a glass fiber. All measurements were made on an Enraf-Nonius CAD4 diffractometer with graphite-monochromated Mo-α radiation. Crystal, data collection, and refinement parameters are given in Table 5.

Cell constants and an orientation matrix for data collection, obtained from a least-squares refinement using the setting angles of 25 carefully centered reflections in the range $10.44 < 2\theta < 18.04°$, corresponded to a primitive monoclinic cell with dimensions $a = 16.743(7)$ Å, $b = 19.458(6)$ Å, $c = 16.859(5)$ Å, $\beta = 119.57(3)°$, and $V = 4776(3)$ Å^3. For $Z = 2$ and FW = 1632.30, the calculated density is 1.13 g/cm^3. Based on the systematic absences of $0k0$, $k = 2n + 1$, packing considerations, a statistical analysis of intensity distribution, and the successful solution and refinement of the structure, the space group was determined to be $P2_1$ (No. 4).

The data were collected at a temperature of -90 ± 1 °C using the $\omega-2\theta$ scan technique to a maximum 2θ value of 52.6°. Scans of $(0.56 + 1.14 \tan\theta)°$ were made at a speed of 1.5−16.0°/min (in ω). Moving-crystal moving counter background measurements were made by scanning an additional 25% above and below the scan range. The counter aperture consisted of a variable horizontal slit with a width ranging from 2.0 to 2.5 mm and a vertical slit set to 2.0 mm. The diameter of the incident beam collimator was 0.7 mm, and the crystal-to-detector distance was 21 cm. For intense reflections, an attenuator was automatically inserted in front of the detector.

Table 5. Data Collection and Refinement Parameters for X-ray Structures of Pd((*R*)-Tol-BINAP)$_2$ (**1b**) and (PPh_3)(Br)Pd[2-diphenylphosphino-2′-yl-1,1′-binaphthyl)] (**6**)

	1b	**6**
empirical formula	$C_{108}H_{92}P_4Pd$	$C_{56}H_{43}BrP_2Pd$
formula weight	1632.30	964.15
crystal color, habit	red plates	yellow block
crystal system	monoclinic primitive	triclinic
lattice parameters	$a = 16.743(7)$ Å $b = 19.458(6)$ Å $c = 16.859(5)$ Å $\beta = 119.57(3)°$	$a = 12.3757(2)$ Å $b = 12.9432(2)$ Å $c = 14.5021(2)$ Å $\alpha = 83.5768(7)°$ $\beta = 82.1315(4)°$ $\gamma = 77.3824(8)°$
volume	4776(3) Å^3	2237.43(6) Å^3
space group	$P2_1$ (No. 4)	$P\bar{1}$
Z value	2	2
diffractometer	Enraf-Nonius CAD-4	Siemens P4/CCD
radiation	Mo Kα ($\lambda = 0.710\ 69$ Å)	Mo Kα ($\lambda = 0.710\ 69$ Å)
T	−90.0 °C	−75(2) °C
residuals	R; R_w 0.053; 0.069	R; R_w 0.0335; 0.0906
goodness-of-fit indicator	1.64	0.985

Of the 10,313 reflections which were collected, 9969 were unique ($R_{int} = 0.062$). The intensities of three representative reflections were measured after every 60 min of X-ray exposure time. No decay correction was applied.

The linear absorption coefficient, μ, for Mo-α radiation is 3.1 cm^{-1}. Azimuthal scans of several reflections indicated no need for an absorption correction. The data were corrected for Lorentz and polarization effects.

The structure was solved by direct methods[102] and expanded using Fourier techniques.[103] The non-hydrogen atoms were refined anisotropically. Hydrogen atoms were included but not refined. In the case of methyl group hydrogen atoms, one hydrogen atom was located in the difference map and included at an idealized distance to set the orientation of the remaining two hydrogen atoms. Four benzene solvent molecules were included and refined at 50% occupancy. The final cycle of full-matrix least-squares refinement[104] was based on 6383 observed reflections ($I > 3.00\sigma(I)$) and 1125 variable parameters and converged (largest parameter shift was 0.02 times its esd) with unweighted and weighted agreement factors of

$$R = \sum||F_o| - |F_c||/\sum|F_o| = 0.053$$

$$R_w = [(\sum w(|F_o| - |F_c|)^2/\sum wF_o^2)]^{1/2} = 0.069$$

The standard deviation of an observation of unit weight[105] was 1.64. The weighting scheme was based on counting statistics and included a factor ($p = 0.040$) to downweight the intense reflections. Plots of $\sum w(|F_o| - |F_c|)^2$ versus $|F_o|$, reflection order in data collection, $\sin\theta/\lambda$, and various classes of indices showed no unusual trends. The maximum and minimum peaks on the final difference Fourier map corresponded to 0.65 and −0.51 e$^-$/Å^3, respectively.

(102) *SIR92*: Altomare, A.; Burla, M. C.; Camalli, M.; Cascarano, M.; Giacovazzo, C.; Guagliardi, A.; Polidori, G. *J. Appl. Crystallogr.* **1994**, in preparation.

(103) *DIRDIF94*: Beurskens, P. T.; Admiraal, G.; Beurskens, G.; Bosman, W. P.; de Gelder, R.; Israel, R.; Smits, J. M. M. The DIRDIF-94 program system, Technical Report of the Crystallography Laboratory, University of Nijmegen, The Netherlands, 1994.

Table 6. Intramolecular Bond Distances (Å) and Angles (deg) for **1b**

Pd(1)−P(1)	2.278(2)	Pd(1)−P(3)	2.278(2)
Pd(1)−P(2)	2.2872(13)		
P(1)−Pd(1)−P(2)	127.90(6)	P(1)−Pd(1)−P(3)	124.02(5)
P(1)−Pd(1)−P(2)	107.80(5)		

Neutral atom scattering factors were taken from Cromer and Waber.[106] Anomalous dispersion effects were included in F_{calc};[107] the values for $\Delta f'$ and $\Delta f''$ were those of Creagh and McAuley.[108] The values for the mass attenuation coefficients were those of Creagh and Hubbel.[109] All calculations were performed using the teXsan[110] crystallographic software package of Molecular Structure Corp.

Bond distances and angles for **1b** are given in Table 6.

X-ray Crystal Structure of [(DPPF)Pd]$_2$(μ-DPPF) (3) and *rac*-(PPh$_3$)(Br)Pd[2′-(diphenylphosphino)-2-yl-(1,1′-binaphthyl)] (6). The single-crystal X-ray diffraction experiment was performed on a Siemens P4/CCD diffractometer. Crystal, data collection, and refinement parameters for **6** are given in Table 5; data for **3** are given in the Supporting Information. Systematic absences and diffraction symmetry are consistent for the space groups $P1$ and P for **3** and $P1$ and $P\bar{1}$ for **6**. The E statistics suggested the centrosymmetric option for both, which yielded chemically reasonable and computationally stable results of refinement. The structures were solved using direct methods, completed by subsequent difference Fourier syntheses, and refined by full-matrix, least-squares procedures. An empirical absorption correction was applied to the data for both **3** and **6** using the program DIFABS. All non-hydrogen atoms were refined with anisotropic displacement coefficients. Hydrogen atoms were treated as idealized contributions. Three molecules of THF cocrystallized with **3**, one of which is disordered over an inversion center. There is one benzene molecule in the asymmetric unit of **6**. Bond distances and angles for **6** are given in Table 7. One of the phenyl rings attached to P(1) of **3** possesses very large thermal ellipsoids in a pattern consistent with positional disorder. The resolution of the current data did not allow the construction of a multisite disorder model.

Table 7. Selected Bond Distances (Å) and Angles (deg) for (PPh$_3$)(Br)Pd[2-diphenylphosphino-2′-yl-1,1′-binaphthyl)] (**6**)

Pd(1)−C(1)	2.010(2)	Pd(1)−Br(1)	2.5141(3)
Pd(1)−P(1)	2.3079(6)	Pd(1)−P(2)	2.3382(6)
P(2)−Pd(1)−C(1)	90.71(7)	P(2)−Pd(1)−P(1)	156.60(2)
P(2)−Pd(1)−Br(1)	93.22(2)	C(1)−Pd(1)−Br(1)	164.27(7)
C(1)−Pd(1)−P(1)	80.02(6)	P(1)−Pd(1)−Br(1)	101.52(2)
C(10)−C(1)−Pd(1)	126.9(2)	C(2)−C(1)−Pd(1)	112.8(2)
C(1)−[Br(1)−Pd(1)−P(2) plane]	164.77°	P(1)−[Br(1)−Pd(1)−P(2) plane]	−129.34°

All software and sources of the scattering factors are contained in the SHELXTL (5.03) program library (G. Sheldrick, Siemens XRD, Madison, WI). The program DIFABS is described by N. Walker and D. Stuart (*Acta Crystallogr.* **1983**, *A39*, 158).

Acknowledgment. We are grateful to the NIH (R29-GM55382-01-035) for support of this work. The University of Delaware acknowledges the National Science Foundation (Grant CHE-9628768) for their support of the purchase of the CCD-based diffractometer.

Supporting Information Available: Figures S1−S7, tables of positional parameters and B(eq), U values, intramolecular distances, intramolecular bond angles, Cartesian coordinates, and torsion or conformational angles for hydrogen and non-hydrogen atoms for **1b**, **3**, and **6** (PDF). This material is available free of charge via the Internet at http://pubs.acs.org.

JA9944599

(104) Least-squares:

Function minimized: $$\sum w(|F_o| - |F_c|)^2$$

where $$w = 4F_o^2/\sigma^2(F_o^2) = [\sigma^2(F_o) + (pF_o/2)^2]^{-1}$$

$$F_o^2 = S(C - RB)/\mathrm{Lp}$$

and $$\sigma^2(F_o^2) = [S^2(C + R^2B) + (pF_o^2)^2]/\mathrm{Lp}^2$$

S = scan rate, C = total integrated peak count, R = ratio of scan time to background counting time, B = total background count, Lp = Lorentz-polarization factor, and p = p-factor.

(105) Standard deviation of an observation of unit weight:

$$[Sw(|F_o| - |F_c|)^2/(N_o - N_v)]^{1/2}$$

where N_o = number of observations and N_v = number of variables.

(106) Cromer, D. T.; Waber, J. T. *International Tables for X-ray Crystallography*; The Kynoch Press: Birmingham, England, 1974; Vol. IV, Table 2.2 A.

(107) Ibers, J. A.; Hamilton, W. C. *Acta Crystallogr.* **1964**, *17*, 781.

(108) Creagh, D. C.; McAuley, W. J. In *International Tables for Crystallography*; Wilson, A. J. C., Ed.; Kluwer Academic Publishers: Boston, 1992; Vol. C, Table 4.2.6.8, pp 219−222.

(109) Creagh, D. C.; Hubbell, J. H. In *International Tables for Crystallography*; Wilson, A. J. C., Ed.; Kluwer Academic Publishers: Boston, 1992; Vol. C, Table 4.2.4.3, pp 200−206.

(110) *teXsan*: Crystal Structure Analysis Package, Molecular Structure Corporation, 1985, 1992.